Biotechnology Letters (2005) 27: 883–891
DOI 10.1007/s10529-005-7176-6
© Springer 2005

Expression and purification of N and E proteins from Severe Acute Respiratory Syndrome (SARS)-associated coronavirus: a comparative study

Chia-Wei Lai[1], Yao-Chi Chung[1], Yiu-Kay Lai[2], Margaret Dah-Tsyr Chang[2] & Yu-Chen Hu[1,*]
[1]*Department of Chemical Engineering, National Tsing Hua University, 300, Hsinchu, Taiwan*
[2]*Institute of Biotechnology, National Tsing Hua University, 300, Hsinchu, Taiwan*
[3]*Institute of Molecular and Cellular Biology, National Tsing Hua University, 300, Hsinchu, Taiwan*
**Author for correspondence (Fax: +886-3-571-5408; E-mail: ychu@mx.nthu.edu.tw)*

Received 13 April 2005; Accepted 5 May 2005

Key words: baculovirus, coronavirus, immobilized metal affinity chromatography, Severe Acute Respiratory Syndrome virus

Abstract

Histidine-tagged N (rNH) and E (rEH) proteins of Severe Acute Respiratory Syndrome (SARS)-coronovirus were expressed in the baculovirus/insect cell system and purified by immobilized metal affinity chromatography. rNH and rEH proteins differed markedly with respect to expression levels, cell death kinetics and subcellular localizations that led to different extraction and purification schemes. The features of both proteins are compared and the potential applications of purified rNH and rEH are discussed.

Introduction

A global outbreak of Severe Acute Respiratory Syndrome (SARS) occurred in 2003 and caused a mortality rate over 10% as of August 2003. The etiologic agent of SARS has been identified as a novel SARS-associated coronavirus (SARS-CoV) whose virions are composed of four proteins: spike (S), envelope (E), membrane (M) and nucleocapsid (N) proteins (Ksiazek *et al.* 2003, Peiris *et al.* 2003). The N protein binds to a defined packaging signal on the RNA, leading to formation of the helical nucleocapsids. The E protein is a minor yet critical structural component in coronavirus assembly because virus-like particles (VLP) can form upon co-expression with M protein, whereas expression of M protein alone does not produce VLP (Bos *et al.* 1996).

Successful control of global SARS epidemic requires vaccines and diagnostic methods for effective prevention and monitoring. The development of either vaccines or diagnostic reagents often requires large quantities of recombinant proteins. Currently, research efforts have mostly been directed toward exploring the potentials of S, M and N proteins for these purposes, but relevant studies concerning the potential of E protein is absent. Although the functions of E protein are partly known, a detailed characterization of E protein has been impeded due to its very low abundance in the virus and in the infected cells. To test the possible applications of E protein as vaccines or diagnostic reagents and to investigate the fundamental roles in pathogenesis, purified E proteins are desired. To address this need, the expression of histidine-tagged SARS-CoV E protein using the baculovirus system and its purification using immobilized metal affinity chromatography (IMAC) are reported here and the proteins are compared with those of SARS-CoV N proteins.

Materials and methods

Chemicals

All chemicals and reagents were obtained from Sigma unless otherwise noted.

Cell and medium

Insect cell Sf-9 line, (*Spodoptera frugiperda)* was propagated and maintained in TNM-FH medium (Gibco BRL, Gaithersburg, MD) as described elsewhere (Hu *et al.* 2002). The cell density was counted by a hemacytometer and the viability was determined by Trypan Blue dye exclusion.

Construction of recombinant plasmids and baculoviruses

The vectors containing the N and E gene fragments of SARS-CoV (TW1 strain, GenBank Accession No. AY291451) were cloned, sequenced and kindly provided by College of Medicine, National Taiwan University. The complete coding regions of N and E genes were amplified by polymerase chain reaction (PCR) using primers incorporating 5′ *Bam*HI and 3′ *Pst*I restriction enzyme sites, and then subcloned into pFastBac HTb vector (Invitrogen, Carlsbad, CA). The cloning yielded fusion genes coding for N (or E) protein with 6 histidine residues (His_6) at the N terminus under the transcriptional control of polyhedrin promoter. The resultant plasmids were designated pBac-NH and pBac-EH, respectively (Figure 1). The recombinant baculoviruses were subsequently generated using Bac-to-Bac system (Invitrogen) as described previously (Hu *et al.* 2003) and designated vBacNH and vBacEH, respectively. The storage, amplification and titration of the recombinant viruses were performed as described elsewhere (Hu *et al.* 2003).

Expression and extraction of the recombinant proteins

Insect cells cultured in the spinner flasks were grown to mid-exponential phase ($1.2–1.4 \times 10^6$ cells/ml) and infected by either vBacNH or vBacEH at multiplicities of infection (MOI) of 10. The recombinant proteins expressed by vBacNH- and vBacEH-infected cells were designated rNH and rEH, respectively. To extract the rNH protein, the infected cells were resuspended in the native binding buffer (NBB = 20 mM phosphate, 500 mM NaCl, pH 7.5) containing 0.1 mg PMSF/ml, sonicated and centrifuged at 4 °C ($10{,}000 \times g$) for 30 min to separate the soluble (lysate) and insoluble (pellet) fractions. The extraction of rEH is detailed below (see Results).

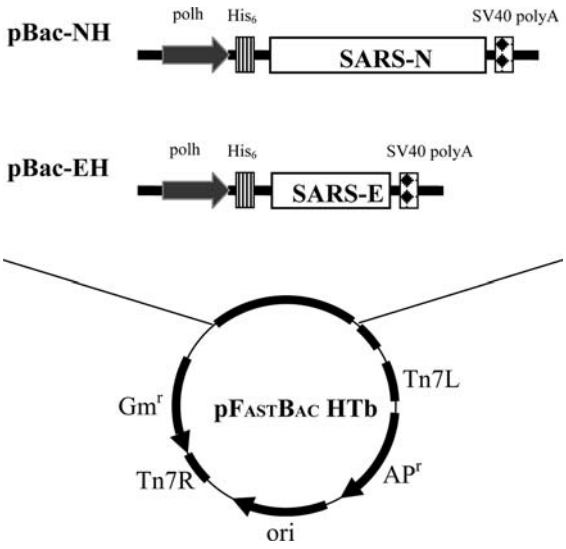

Fig. 1. Schematic illustration of the recombinant baculovirus vectors, pBac-NH and pBac-EH, which harbored the gene fragments encoding the SARS-CoV N and E proteins, respectively. Both genes were fused with a His_6 tag at the N-terminus and expressed under the control of polyhedrin (polh) promoter.

SDS-PAGE and Western blot

The proteins released from vBacNH- and vBacEH-infected cells were resolved on 12 and 16.5% (v/v) SDS-PAGE gels, respectively. For rEH protein, Tricine gel system was used to enhance the resolution at low molecular weight (Schagger & von Jagow 1987). After electrophoresis, the gels were either stained by Coomassie Brilliant Blue, or transferred to nitrocellulose membranes for Western blot analysis following standard procedures (Bio-Rad Laboratories, Carlsbad, CA). For Western blot, the primary antibody was mouse anti-His_6 MAb (1:1500 dilution, Amersham Biosciences, London, UK),

while the secondary antibody was goat anti-mouse IgG conjugated to alkaline phosphatase (1:1000 dilution, Kirkegaard and Perry Laboratories, Gaithersburg, MD). Color development was achieved by BCIP/NBT (5-bromo-4-chloro-3-indolyl phosphate/Nitro Blue tetrazolium) color development reagent (Sigma). The scanning densitometry was performed by scanning the gels or membranes and quantifying by Scion Image Shareware (Scion Corporation, Gaithersburg, MD). Purified proteins were serially diluted for the construction of standard curves.

Confocal microscopy

The subcellular localizations of rNH and rEH proteins were examined by confocal microscopy. Briefly, the cells were cultured on sterile cover slips and were infected by vBacNH or vBacEH. Two days after infection, the cells were fixed by methanol/acetone (1:1 v/v) for 5 min at −20 °C, rinsed with phosphate-buffered saline (PBS) and then blocked with 2% bovine serum albumin in PBS for 30 min at 37 °C. The nuclear staining was first performed by labeling with SYBR Green I (1:40,000, Bio-Whittaker, Walkersville, Maine) for 1 h at 37 °C. The proteins were subsequently labeled by mouse anti-His_6 MAb (1:300, Amersham Bioscience) and Cy3-conjugated anti-mouse MAb (1:50, Sigma). The cells were washed 3 times by PBS between labeling steps. The protein localizations were visualized by a confocal microscope (TCS SP2, Leica, Germany).

Purification of the recombinant proteins by IMAC

The recombinant proteins were fused with His_6 tags and thus were purified by IMAC using an FPLC (ÄKTA FPLC, Amersham Biosciences). The resin (Sepharose Fast Flow Gel, Amersham Biosciences) was first coupled with Ni^{2+}. To purify rNH protein, the column was equilibrated with NBB buffer, followed by the loading of lysates into the column at 1 ml/min for 3 cycles. The column was washed by 10 ml NBB buffer containing 20, 50 and 100 mM imidazole to remove non-specifically bound proteins. Higher imidazole concentrations (200, 300 and 500 mM) in the binding buffer were similarly used to elute the desired rNH. To purify rEH protein, the coupled resin was equilibrated with buffer A (20 mM Tris, 50 mM NaCl, 8 M urea, 0.1% Tween 20, pH 7.5), followed by the loading of solublized rEH proteins onto the column at 1 ml/min for 3 cycles. The bound rEH proteins were washed with a linear gradient of urea from 8 to 0 M by mixing buffer A and buffer B (20 mM Tris, 50 mM NaCl, 0.1% Tween 20, pH 7.5) to facilitate refolding. The refolded proteins were then washed and eluted using buffer B containing increasing imidazole concentrations (20, 100, 200, 300 and 500 mM).

One ml of each fraction was monitored at 280 nm and fractions having peak values were further subjected to SDS-PAGE and Western blot analyses. The purified proteins were pooled, dialyzed against PBS overnight at 4 °C and measured for protein concentration using a protein assay kit (Bio-Rad Laboratories).

Results

Expression and subcellular localization of the recombinant proteins rNH and rEH

The correct constructions of vBacNH and vBacEH were checked by DNA sequencing (not shown). To confirm the proper expression of rNH and rEH, Sf-9 cells were infected by vBacNH and vBacEH individually (MOI 10), harvested at 96 h post-infection (hpi), and lysed using the NBB buffer. After centrifugation, the pellets and lysates were analyzed by Western blots using anti-His_6 MAb. As shown in Figure 2, the lysate of vBacNH-infected cells

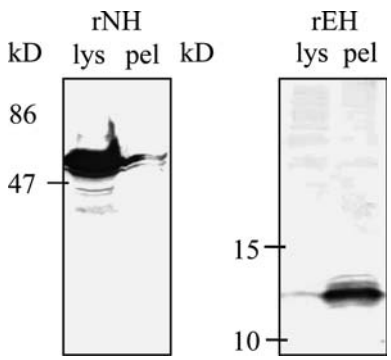

Fig. 2. Western blot analyses of rNH and rEH expressed in insect cells. The cells were lysed in the NBB buffer and centrifuged to separate the lysates (lys) and the pellets (pel).

contained a ≈50 kDa protein, while the pellets of vBacEH-infected cells contained a ≈12 kDa protein. The molecular masses of the expressed proteins agreed well with the projected molecular masses of rNH (49.3 kDa) and rEH (11.6 kDa), indicating the successful expression of both proteins. The majority of rNH was detected in the lysate, whereas rEH was almost exclusively found in the pellet portion.

To examine whether the subcellular localizations of rNH and rEH differed, the proteins were labeled by antibodies and visualized by confocal microscopy. As shown, the nucleus as stained by SYBR Green I (Figure 3a) co-localized with rNH as stained by Cy3-conjugated secondary MAb (Figure 3b), as evidenced by the orange nuclei shown in the merged photograph (Figure 3c). The confocal microscopy thus demonstrated that rNH was mainly located within the nuclei of baculovirus-infected insect cells. In contrast, rEH appeared to reside within the cytoplasm because rNH (strong red dots in Figure 3e) surrounded the nucleus (green dots in Figure 3f). Considering that the vast majority of rEH remained associated with cell pellets after initial sonication and centrifugation, rEH appeared to anchor on the membranes of certain organelles.

Extraction of rEH

Since rEH was tightly bound to the pellets, a two-stage extraction scheme was adopted in order to recover rEH more efficiently. In the first stage, the cellular proteins were released using normal lysis buffer (40 mM Tris/HCl, 300 mM NaCl, 5 mM EDTA, 1% Triton X-100, 0.1 mg PMSF/ml, pH 7.5) and separated from the insoluble fractions by centrifugation. In the second stage, the pellets were resuspended in the high salt lysis buffer (50 mM Tris/HCl, 1 M NaCl, 5 mM EDTA, 0.1 mg PMSF/ml, pH 7.5) and sonicated (X). Alternatively, the pellets were resuspended in the high salt lysis buffer containing 40 mM detergents [*n*-dodecyl-β-maltoside (DOM), Chapso, *n*-octyl-β-glucoside (OG), and Igepal-630] or in the low salt lysis buffer (20 mM Tris/HCl, 50 mM NaCl, 0.1 mg PMSF/ml, pH 7.5) containing 8 M urea, sonicated for 1 min, and centrifuged. Both the supernatant (s) and the pellet (p) fractions were subjected to Western blot analysis.

As shown in Figure 4, all the rEH proteins remained in the pellets (p) after the first stage extraction (lanes 1 and 2), but many cellular proteins were extracted and removed as revealed by

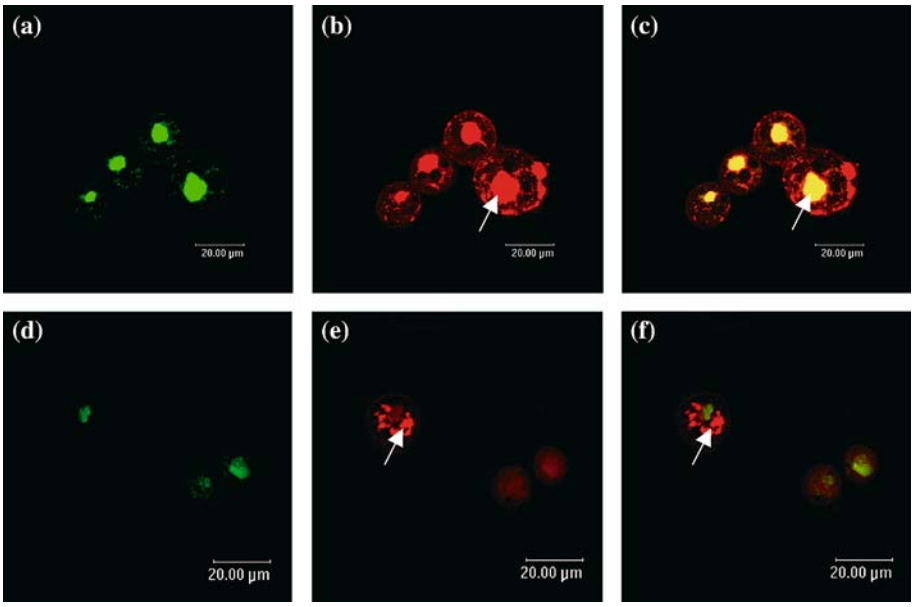

Fig. 3. Confocal microscopy imaging of cells infected by vBacNH (a–c) and vBacEH (d–f) at MOI 10. The nuclei were labeled by SYBR Green I while rNH and rEH proteins were first labeled with anti-His_6 mouse MAb, followed by labeling with Cy3-conjugated anti-mouse MAb. The localizations of rNH (b) and rEH (e) are indicated by the strong red fluorescence and arrows. The merged photographs are shown in (c) and (f).

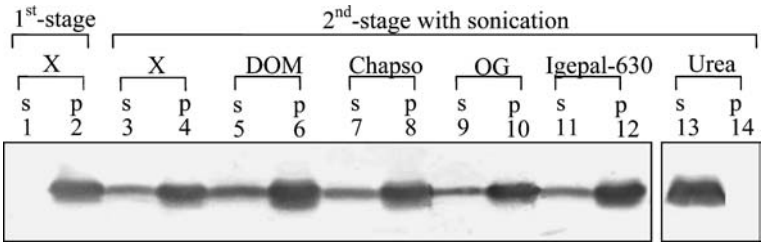

Fig. 4. Western blot analyses of rEH extracted by a two-stage process. The cells were infected by vBacEH at MOI 10 and harvested at 3 dpi. In the first stage, the cells were lysed using the normal lysis buffer, and then the lysates were separated from the insoluble fractions by centrifugation. In the second stage, the pellets were resuspended in the high salt lysis buffer and sonicated (X). Alternatively, the pellets were resuspended in the high salt lysis buffer containing 40 mM detergents (DOM, Chapso, OG and Igepal-630) or in the low salt lysis buffer containing 8 M urea, sonicated, and then the supernatants (s) and pellets (p) were separated for Western blots.

PAGE (not shown). In the second stage, further extensive sonication (lanes 3 and 4) resulted in limited extraction as more proteins were still found in the pellet (p) than in the supernatant (s). Combined with sonication, addition of detergents (lanes 5–12) only partially assisted the solubilization, even though these detergents were commonly used for membrane protein solubilization. Only the urea-containing buffer, in conjugation with sonication in the second stage, fully extracted rEH into the supernatant (lanes 13 and 14). Therefore, this protocol was utilized for all subsequent experiments.

Kinetics of cell death and protein expression

After finalizing the extraction protocols, the time-course profiles of cell viability and protein expression were examined. As shown in Figure 5a, the viability of vBacNH-infected cells remained high at 2 dpi and dropped more rapidly at 3 and 4 dpi, which was typical of baculovirus infection (Hu & Bentley 2001) and suggested that the rNH expression imposed little or no influence on the cell viability. In contrast, the viability of vBacEH-infected cells started to decrease precipitously at 2 dpi, and significantly dropped to ≈23% at 3 dpi. Furthermore, the rNH expression commenced at 1 dpi, rapidly reached the maximum at 3 dpi, and declined thereafter (Figure 5b, upper panel). In contrast, the rEH expression started at 2 dpi and remained at the plateau until 5 dpi (Figure 5b, lower panel). Collectively, the cells infected by vBacNH and vBacEH exhibited different death and expression kinetics.

Purification by IMAC

Since rEH and rNH possessed rather distinct properties, the purification schemes by IMAC were customized individually. Because rNH protein was readily soluble in the NBB buffer, rNH was purified by IMAC under native conditions and the samples collected during the purification were checked by Western blot (Figure 6a) and

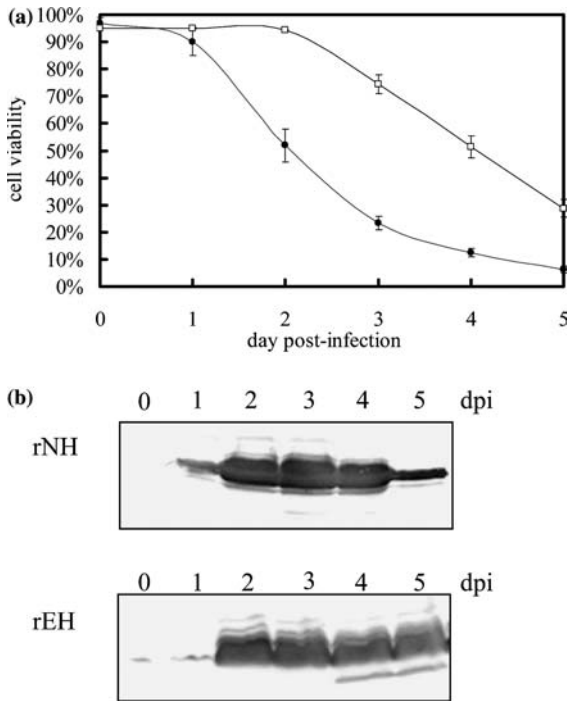

Fig. 5. Time-course profiles of cell viability and expression level. (a) Viabilities of cells infected by vBacNH (□) and vBacEH (●). The data represent the mean ± standard deviations of 3 independent experiments. (b) Western blot analysis of the rNH and rEH expression over time post-infection.

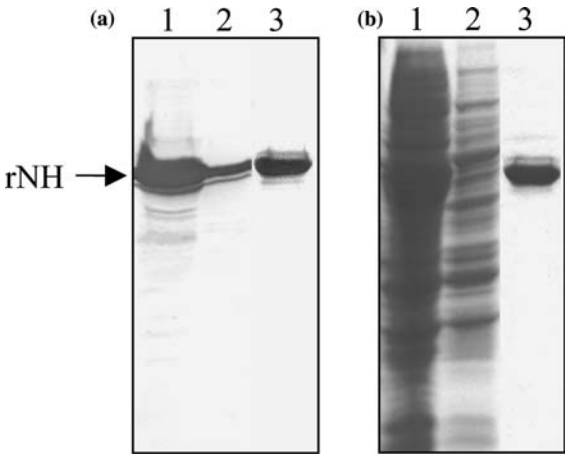

Fig. 6. Western blot (a) and SDS-PAGE (b) analyses of rNH proteins purified by IMAC. Lane 1, cell lysate; lane 2, flow through; lane 3, the sample eluted by 200 mM imidazole buffers.

SDS-PAGE (Figure 6b). Comparing to the crude sample (lane 1), a relatively low percentage of rNH protein flowed through the column (lane 2), indicating a strong binding. After step wishes using buffers containing 20, 50 and 100 mM imidazole (not shown), abundant 50 kDa proteins were eluted by 200 mM imidazole as revealed by Western blot (lane 3, Figure 6a). Further increases in imidazole concentrations to 300 and 500 mM eluted no more proteins (not shown). The SDS-PAGE and the densitometry revealed that the purity was higher than 90% and the protein assays further revealed that ≈2.7 mg rNH protein was purified from 100 ml infected cells.

On the other hand, rEH was denatured in the extraction step, hence it was purified under denaturing conditions by employing the extraction buffer for binding. To further enhance binding, 0.1% Tween 20 was added. After binding and initial wash using the urea-containing buffer, a refolding step utilizing a linear gradient between 8 and 0 M urea was implemented prior to further wash and elution. The Western blot (Figure 7a) shows that the binding of rEH to the resin was satisfactory with the aid of Tween 20 because relatively smaller amounts of rEH flowed through the column (lane 2). The binding remained strong after lowering the urea concentration to zero (lane 3) and increasing the imidazole concentration to 20 and 100 mM (lanes 4 and 5), as no rEH was detected in these fractions. No rEH was eluted by 200 and 300 mM imidazole buffers either (not shown). The rEH proteins were finally eluted by 500 mM imidazole buffers (lane 6). The purity was estimated by SDS-PAGE (Figure 7b) and scanning densitometry to be 72%. Protein assays further revealed that ≈0.66 mg rEH protein was recovered from 200 ml infected cells.

Discussion

In this study, we report the expression and purification of histidine-tagged N and E proteins of SARS-CoV. These two proteins exhibited striking differences in expression levels and physical properties which, in turn, affected the purifica-

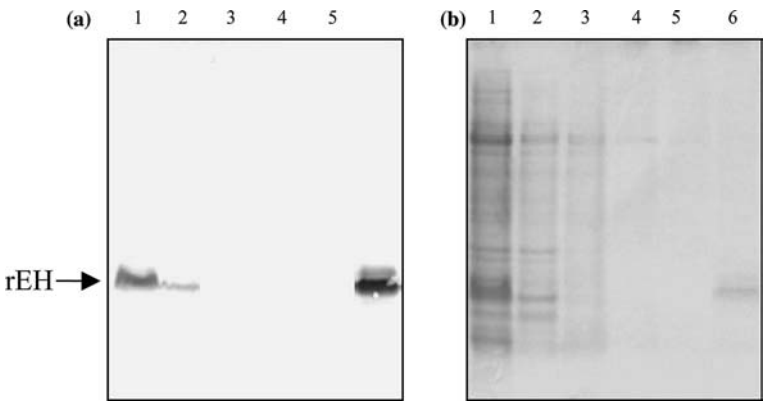

Fig. 7. Western blot (a) and SDS-PAGE (b) analyses of rEH proteins purified by IMAC. Lane 1, cell lysate; lane 2, flow through; lane 3, the sample eluted during the refolding step; lanes 4–6, the samples eluted by 20, 100 and 500 mM imidazole buffers.

tion schemes. The N protein is a major constituent of the coronavirus virion and can be expressed to high levels in the cytoplasm and nucleolus of insect cells (Ren *et al.* 2004). Our confocal microscopy data confirmed that the majority of rNH protein was localized within the nucleus. Such protein is very suitable for expression using the baculovirus/insect cell system as the yield of other similar viral proteins is very high (Hu *et al.* 2002). It is therefore not surprising that our specific yield of rNH amounted up to ≈90 μg/10^6 cells at 3 dpi as estimated by scanning densitometry. On the other hand, the E protein of other coronaviruses is present in minute amounts on the envelope, and is reported to target to the Golgi complex (Corse & Machamer 2000). Our confocal microscopy data and the finding that rEH is tightly bound to intracellular membranes also support this notion. The excessive overexpression of such membrane protein inevitably undermines the secretion, sorting and modification of cellular proteins, hence the maximum specific yield of rEH protein was only 12.5 μg/10^6 cells at 3 dpi as estimated by densitometry, which was ≈7-fold lower compared to rNH protein.

It is also interesting to note that the vBacEH-infected cells exhibited faster death rates than the vBacNH-infected cells. The onset of rEH expression was concurrent with the dramatic decrease in viability, implying a correlation between the rEH expression and cell viability. Therefore, the quick drop of viability was originally deemed a result of apoptosis induced by rEH protein because the E protein of mouse hepatitis virus (also a coronavirus) induces apoptosis in cultured cells (An *et al.* 1999). However, no signs of DNA fragmentation, a characteristic of apoptosis, were observed in the vBacEH-infected cells even at 3 dpi (unpublished observation). Another possibility to account for the rapid death is that rEH protein permeabilized the cell membrane, caused the infiltration of Trypan Blue dye, and contributed to the rapid "cell death", because SARS-CoV E protein was recently suggested to be a viroporin that can alter the membrane permeability upon expression in *E. coli* (Liao *et al.* 2004).

The amino acid sequence analysis revealed that SARS-CoV N protein is basic, highly charged, and has a low hydropathicity (data not shown). These properties contributed to its high solubility in the NBB buffer which, in turn, enabled simple purification of rNH protein in a single step using IMAC. In marked contrast, SARS-CoV E protein contains a transmembrane domain (aa 12–34) that forms an unusual palindromic helical hairpin around a pseudo-center of symmetry (Arbely *et al.* 2004). Furthermore, SARS-CoV E protein was recently suggested to form cation-selective ion channels in planar lipid bilayers (Wilson *et al.* 2004), which supports the notion that SARS-CoV E protein forms an oligomer (Liao *et al.* 2004). These characteristics might account for its strong propensity to associate with the membrane. Albeit uncommon, such oligomer could have formed detergent-resistant structures (Weisz *et al.* 1993, Sevier & Machamer 1998), so that the detergents commonly used for solubilizing integral membrane proteins failed to completely solubilize rEH. In this study, we have tested parameters such as salt concentrations (0.15–1 M NaCl), sonication time (0.5–1.5 min per 0.5 ml solution), incubation time (30 min to overnight) (data not shown) and detergent types (see Figure 4) in order to extract rEH from the pellets more efficiently, but only a limited degree of success was achieved. The rEH protein could only be completely released from the cellular pellets when a two-stage process incorporating 8 M urea in the second stage was adopted. One benefit of this process was that lots of other soluble, contaminating materials were removed in the first stage, thus reducing the complexity in the subsequent IMAC purification.

The unusual properties of rEH also imparted considerable difficulties in purification. Initially, the binding was poor when high salt (500 mM NaCl) Tris buffers were used, hence non-ionic detergents (e.g. DOM, Chapso, OG and Tween 20) were added (Porath & Olin 1983) and all of which significantly improved binding (data not shown). With this treatment, however, the binding became so strong that considerable amounts of rEH remained stuck to the resin. Even low pH (e.g. 4) or high imidazole concentration (up to 1 M) failed to elute rEH completely off the column (data not shown). Thus the salt concentration was lowered to 50 mM to decrease the ionic strength and enhance elution. In conjunction with an on-column refolding step, the final protocol resulted in the recovery of ≈0.66 mg purified rEH from 2×10^8 cells (Figure 7).

For the control of SARS transmission, rapid and accurate diagnosis in the early phase of infection is crucial. Equally important is the development of vaccines and antiviral drugs to prevent or treat the disease. Among the known SARS-CoV proteins, N protein has been demonstrated to be a valuable marker for early detection of SARS-CoV infection (Che *et al.* 2004). Furthermore, recent publications have suggested that N protein is involved not only in capsid assembly, but also in the activation of AP1-pathway (He *et al.* 2003) and in the induction of apoptosis in COS-1 cells (Surjit *et al.* 2004), indicating that N protein may serve as a target molecule for the development of vaccine or antiviral drugs. On the other hand, the roles of E protein are poorly characterized comparing to S, M and N proteins, probably due to its small size and low abundance in the virions. Although SARS-CoV E protein is shown to form ion channels, whether the ion channel activity is involved in the known physiological roles remains to be investigated. Also, SARS-CoV E protein is recently suggested to be a viroporin, disruption of the E protein functions thus may possibly abrogate viral infectivity, rendering SARS-CoV E protein a potential target for the development of antiviral drugs. All these together further substantiate the importance of producing and purifying SARS-CoV N and E proteins in the heterologous expression system. Although many reports concerning the expression and purification of SARS-CoV N protein have been published, however, the expression of SARS-CoV E protein in the eucaryotic system and its purification have yet to be reported, probably due to its lower expression level and extra difficulty in purification. Our system thus provides a tool for the expression and purification of SARS-CoV E protein and may facilitate the development of diagnostic kits, vaccines or antiviral drugs against SARS.

Acknowledgement

We thank Dr. Pei-Jer Chen (College of Medicine, National Taiwan University) for providing vectors harboring the N and E genes, and Prof. Sung, Shin-Wen and Chen, Sung-Chin (Department of Chemical Engineering, National Tsing Hua University) for technical assistance in confocal microscopy. We are also grateful to the financial support from the National Science Council (NSC 92-2751-B-007-001-Y and NSC93-2213-E-007-104).

References

An S, Chen CJ, Yu X, Leibowitz JL, Makino S (1999) Induction of apoptosis in murine coronavirus-infected cultured cells and demonstration of E protein as an apoptosis inducer. *J. Virol.* **73**: 7853–7859.

Arbely E, Khattari Z, Brotons G, Akkawi M, Salditt T, Arkin IT (2004) A highly unusual palindromic transmembrane helical hairpin formed by SARS coronavirus E protein. *J. Mol. Biol.* **341**: 769–779.

Banerjee P, Joo JB, Buse JT, Dawson G (1995) Differential solubilization of lipids along with membrane proteins by different classes of detergents. *Chem. Phys. Lipids* **77**: 65–78.

Bos EC, Luytjes W, van der Meulen HV, Koerten HK, Spaan WJ (1996) The production of recombinant infectious DI-particles of a murine coronavirus in the absence of helper virus. *Virology* **218**: 52–60.

Che XY, Hao W, Wang YD, Di B, Yin K, Xu YC, Feng CS, Wan ZY, Cheng VCC, Yuen KY (2004) Nucleocapsid protein as early diagnostic marker for SARS. *Emerg. Infect. Dis.* **10**: 1947–1949.

Corse E, Machamer CE (2000) Infectious bronchitis virus E protein is targeted to the Golgi complex and directs release of virus-like particles. *J. Virol.* **74**: 4319–4326.

He RT, Leeson A, Andonov A, Li Y, Bastien N, Cao JX, Osiowy C, Dobie F, Cutts T, Ballantine M, Li XG (2003) Activation of AP-1 signal transduction pathway by SARS coronavirus nucleocapsid protein. *Biochem. Biophys. Res. Commun.* **311**: 870–876.

Hu Y-C, Bentley WE (2001) Effect of MOI ratio on the composition and yield of chimeric infectious bursal disease virus-like particles by baculovirus co-infection: deterministic predictions and experimental results. *Biotechnol. Bioeng.* **75**: 104–119.

Hu Y-C, Hsu T-A, Huang J-H, Ho M-S, Ho Y-C (2003) Formation of enterovirus-like particle aggregates by recombinant baculoviruses co-expressing P1 and 3CD in insect cells. *Biotechnol. Lett.* **25**: 919–925.

Hu Y-C, Liu H-J, Chung Y-C (2002) High level expression of the key antigenic protein, σC, from avian reovirus into insect cells and its purification by immobilized metal affinity chromatography. *Biotechnol. Lett.* **24**: 1017–1022.

Ksiazek TG, Erdman D, Goldsmith CS, Zaki SR, Peret T, Emery S, Tong S, Urbani C, Comer JA, Lim W, Rollin PE, Dowell SF, Ling AE, Humphrey CD, Shieh WJ, Guarner J, Paddock CD, Rota P, Fields B, DeRisi J, Yang JY, Cox N, Hughes JM, LeDuc JW, Bellini WJ, Anderson LJ (2003) A novel coronavirus associated with severe acute respiratory syndrome. *New Engl. J. Med.* **348**: 1953–1966.

Liao Y, Lescar J, Tam JP, Liu DX (2004) Expression of SARS-coronavirus envelope protein in *Escherichia coli* cells alters membrane permeability. *Biochem. Biophys. Res. Commun.* **325**: 374–380.

Peiris JSM, Lai ST, Poon LLM, Guan Y, Yam LYC, Lim W, Nicholls J, Yee WKS, Yan WW, Cheung MT, Cheng VCC, Chan KH, Tsang DNC, Yung RWH, Ng TK, Yuen KY

(2003) Coronavirus as a possible cause of severe acute respiratory syndrome. *Lancet* **361**: 1319–1325.

Porath J, Olin B (1983) Immobilized metal ion affinity adsorption and immobilized metal ion affinity chromatography of biomaterials. Serum protein affinities for gel-immobilized iron and nickel ions. *Biochemistry* **22**: 1621–1630.

Ren AX, Xie YH, Kong YY, Yang GZ, Zhang YZ, Wang Y, Wu XF (2004) Expression, purification and sublocalization of SARS-CoV nucleocapsid protein in insect cells. *Acta Biochim. Biophys. Sin.* **36**: 754–758.

Schagger H, von Jagow G (1987) Tricine-sodium dodecyl sulfate-polyacrylamide gel electrophoresis for the separation of proteins in the range from 1 to 100 kDa. *Anal. Biochem.* **166**: 368–379.

Sevier CS, Machamer CE (1998) Fragmentation of a Golgi-localized chimeric protein allows detergent solubilization and reveals an alternate conformation of the cytoplasmic domain. *Biochemistry* **37**: 185–192.

Surjit M, Liu B, Jameel S, Chow VT, Lal SK (2004) The SARS coronavirus nucleocapsid protein induces actin reorganization and apoptosis in COS-1 cells in the absence of growth factors. *Biochem. J.* **383**: 13–18.

Weisz OA, Swift AM, Machamer CE (1993) Oligomerization of a membrane protein correlates with its retention in the Golgi complex. *J. Cell Biol.* **122**: 1185–1196.

Wilson L, McKinlay C, Gage P, Ewart G (2004) SARS coronavirus E protein forms cation-selective ion channels. *Virology* **330**: 322–331.